AC 2009-1584: RECONCILIATION OF BERNOULLI'S EQUATION IN CHANNEL FLOW: AN IN-DEPTH EMPIRICAL AND NUMERICAL APPROACH

Jordon Schultz, Rochester Institute of Technology
Senior in the Mechanical Engineering Technology Program

Larry Villasmil, Rochester Institute of Technology

Reconciliation of Bernoulli's Equation in Channel Flow: An In-Depth Empirical and Numerical Approach. Part I

This paper revolves around the investigation process of a peculiar flow phenomenon occurring during Bernoulli's principle experiments. Moreover, the experiment is aimed at demonstrating both the conservation of energy principle and the continuity equation. In the past, students have struggled to obtain meaningful results when evaluating the variation of total energy in the system. Some have concluded that the experiment is an exercise in futility and stated that head losses cannot be calculated to any degree of accuracy. Over a ten-week period, experiments were run in both laminar and turbulent flow regimes, and the experimental environment was thoroughly cleaned. Flow visualizations were performed using black ink to observe the fluid flow behavior, and predictions were adjusted for the observed differing rate of energy conversion. Lower wall friction was introduced into head loss equations, and the diverging flow area was adjusted for an observed re-circulation zone. After determining the throat of the channel as the source of the strange phenomenon, 2D numerical simulations were attempted, but not completed, using commercial CFD software, so the numerical approach will be the subject of a second paper. Overall, this paper will reveal the complexity of fluid flow through a converging-diverging channel, and highlight the experimental process involved that was used to elucidate peculiar phenomenon. Lastly, this paper will be used as the seminal work for an advanced course in applied fluid mechanics for engineering technology students.

Nomenclature

Variable	Units	Description	Variable	Units	Description
P_H	m	Pressure head	V_H	m	Velocity head
H	m	Fluid manometer height	R	m	Hydraulic radius
A	mm^2	Cross sectional area	ε	m	Surface roughness factor
h	mm	Channel height	N_R	-	Reynolds number
t	mm	Channel width	η	$N*s/ m^2$	Dynamic viscosity
V	m/s	Velocity	ρ	Kg/m^3	Density
Q	L/min	Flow rate	ΔL	m	Length between taps
T_H	m	Total head	HL_{TC}	m	Cumulative theoretical head loss
g	m/sec^2	Acceleration due to gravity	HL_T	m	Theoretical head loss
I_H	m	Ideal head	θ	Deg.	Angle of channel incline
HL	m	Experimental head loss			
HLC	m	Cumulative experimental head loss			
HLN	m	Non-cumulative experimental head loss			

Introduction

The Bernoulli flow experiment has been used at Rochester Institute of Technology for many years. It is a staple experiment performed by senior students in the Thermofluids Laboratory course. In the past, students have expressed frustration in obtaining meaningful results from the experiment. Some past students have called it “an exercise in futility,” and others have failed to use the raw data in meaningful ways. Other students have even suggested changing the design of the channel to a circular cross section. This investigation was performed to elucidate an interesting phenomenon observed when analyzing the raw data. Moreover, this investigation will help future students better understand the experiment, and it will be used in an advanced fluid mechanics course for engineering technology students.

The experimental procedure is typically performed by first obtaining a steady fluid level in the inlet tank, and then various flow rates can be obtained by adjusting an outlet pipe. After obtaining a steady flow rate, students typically record the water height in 11 manometer taps equally spaced along the length of the channel. Next, the fluid is allowed to collect in a basin whereby the volumetric flow rate is recorded using a clear sight glass with a scale and a stopwatch. This is typically done several times, and the average volumetric flow rate is then calculated. When analyzing the raw data, students typically plot the change in pressure head vs. distance for the various turbulent flow rates. Students also plot the change in kinetic energy vs. distance.

This investigation beganafter evaluating the total energy, ideal head and calculated head losses. Calculated head losses decrease after the channel throat and in turbulent flow become negative. This is not expected, because the fluid cannot convert kinetic energy into pressure energy without appreciable positive head losses. Several experiments were then performed along with attempting numerical simulations to investigate and elucidate this phenomenon. Next, the experiments and their results will be discussed. The process of determining the root of the strange results and the current status of the project will also be outlined.

Initial Experiment

The first step in this investigation was to run the Bernoulli flow experiment “as-is” and attempt to replicate the results of past students. Figure 1 shows the P6231 Bernoulli apparatus along with the test bench. The P6100 hydraulics bench consists of: P6103 constant head inlet tank, P6104 variable head outlet tank, variable speed centrifugal pump, and volumetric measurement tank. Initially, a total of eight different flow rates were run, and each consisted of five volumetric flow rate trials. This was done in an effort to eliminate any measurement errors that could occur while reading the volume sight glass. The manometer heights were recorded for each flow rate using the 1/16th inch scale on the Bernoulli apparatus. Figure 2 shows a section view of the apparatus with the numbered manometer taps. The fluid enters on the left side of the channel from the P6103 inlet tank, then travels from taps 1 to 11 and finally exits into the P6104 outlet tank.

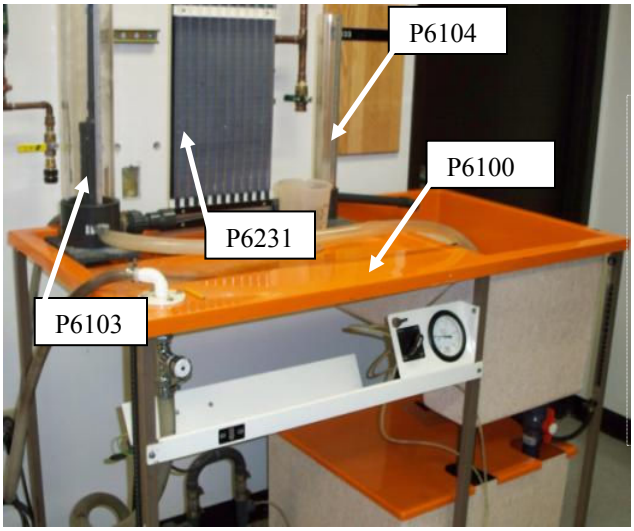

Fig. 1 P6231 Bernoulli apparatus and P6100 hydraulics bench

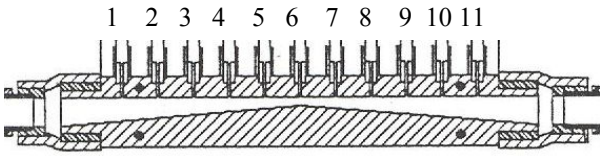

Fig. 2 Section view of P6231 Bernoulli apparatus (1)

After collecting the raw data, a series of initial calculations were performed, and several data products were produced. Initially, the results in the turbulent flow regime are as expected. Figure 3 shows the varying head along the length of the channel. As the fluid enters and moves through the converging section, its kinetic energy increases as a function of channel height. This increase in kinetic energy must be compensated for by a decrease in pressure energy as defined by the simplified Bernoulli's equation, equation 1. Figure 3 shows the change in pressure head along the channel for various flow rates.

Equation 1: $\frac{P}{\gamma}+\frac{V^2}{2\cdot g}=\mathrm{K}$ where $\frac{P_i}{\gamma}=P_{H_i}=H_i$ $i=1,2,...11$

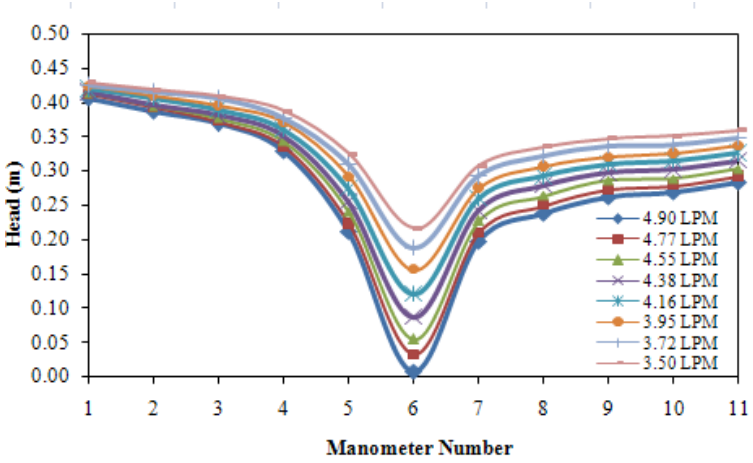

Fig. 3 Change in pressure head along channel length

As expected, the fluid experiences the lowest pressure at manometer 6 (the throat) and gradually recovers the pressure energy as the fluid then diverges. Close examination of the graph reveals that the fluid does not recover all of its original pressure energy, thus appreciable head losses must be accounted for. Another interesting observation of figure 3 is that the fluid does not convert pressure energy into kinetic at the same rate it converts kinetic to pressure energy. This can be seen in the different slopes in the converging and diverging sections of the channel. At the given flow rates, Reynolds numbers vary from a minimum of 5186 at the inlet of the channel to a maximum of 12,603 at the channel throat.

After graphing the change in pressure energy, the total head and ideal head were found at each manometer and plotted. The cross-sectional areas at each manometer tap were calculated using the channel heights shown in figure 4, a channel thickness of 6.35mm, and equation 2. Figure 5 shows the total head and its overall decreasing trend over the channel. Total head is the sum of the pressure head and velocity head at each tap (see equations 3 and 4), thus it would be expected that an overall decrease in total head would occur. Ideal pressure head is shown in figure 6 and is equal to the algebraic difference of the total starting head and the velocity head at each manometer as shown in equation 5. The ideal head represents a total recovery of pressure energy; thus it is symmetric about the throat of the channel.

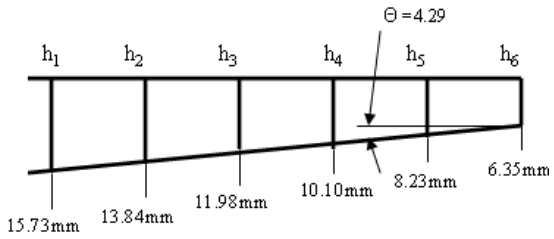

Equation 2: $A_i = h_i \cdot t$

Fig. 4 Channel Heights at manometer taps

Equation 3: $V_i = \frac{Q}{A_i}$ Equation 4: $T_{H_i} = P_{H_i} + \frac{V_i^2}{2 \cdot g}$ Equation 5: $I_{H_i} = T_{H_1} - \frac{V_i^2}{2 \cdot g}$

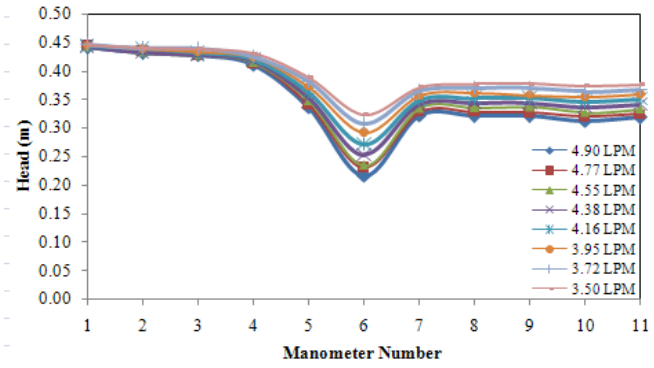

Fig. 5 Total Head

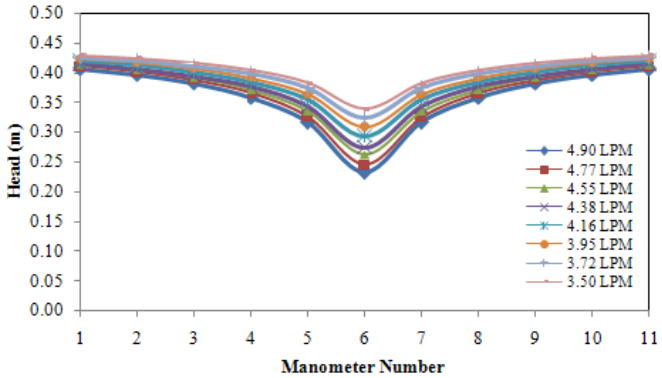

Fig. 6 Ideal Head

Equation 6: $HLC_i = T_{H_1} - P_{H_i}$ Equation 7: $HLN_{i+1} = HL_{i+1} - HL_i$

The experimental head losses were found using equations 6 and 7, cumulative and non-cumulative, as shown above. Figure 7 shows the cumulative head losses in the channel, and the trend appears to be normal from taps 1 through 6. The head losses increase as the fluid increases in velocity and decrease as the fluids speed is reduced in the diverging half of the channel. However, because figure 7 is cumulative, a decrease in head losses should be represented by a smaller positive slope. This is not what figure 7 shows after manometer 6, and it can be postulated that negative head losses have been calculated. A better understanding of the negative head losses can be seen in figure 8. The head losses in each flow rate sharply decrease and become negative after the throat.

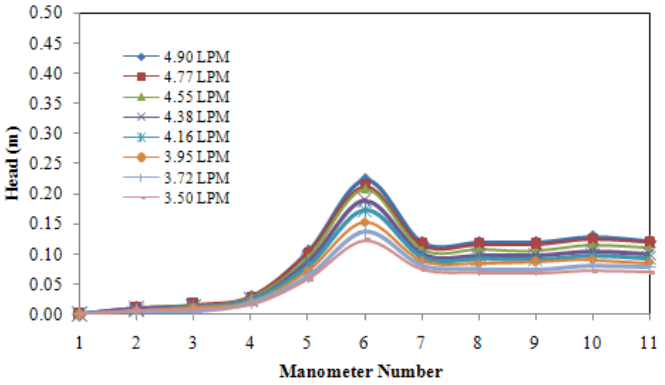

Fig. 7 Cumulative head losses

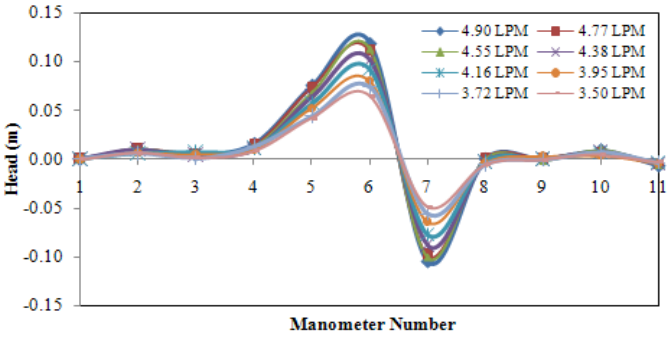

Fig. 8 Non-cumulative head losses

Oddly, the losses then return to zero and do not change from taps 8 and 9. Furthermore, these graphs indicate normal behavior in the converging half of the channel and abnormal fluid behavior in the throat and diverging half. Negative head losses suggest that energy is being introduced into the system or that there is another phenomenon happening that is not yet understood.

Controlling the Experimental Environment

After obtaining strange results, it was hypothesized that an uncontrolled experimental environment may be introducing error. Some possible sources of experimental error were observed, possibly leaks in the constant head inlet tank, the Bernoulli apparatus not being level, and debris in the Bernoulli channel and manometer tap inlets. To further explore these areas, the Bernoulli apparatus was removed from the test bench and disassembled. An observable amount of debris was found inside the apparatus, and it was completely cleaned. While cleaning the device, special care was given to ensure that the manometer inlet holes were completely clean and clear of debris. In some cases, a considerable amount of black debris was removed from the manometer tap inlet holes. Figure 9 shows the debris in the converging half of the channel.

After cleaning both the apparatus and test bench, the Bernoulli apparatus was checked to ensure the inlet and outlet were leveled. Figure 10 shows an image of the apparatus before it was adjusted. This small incline could have added potential energy to the fluid, and it was not detectable to the naked eye. Two-millimeter-thick shims were added to the diverging end of the channel to achieve a level reading.

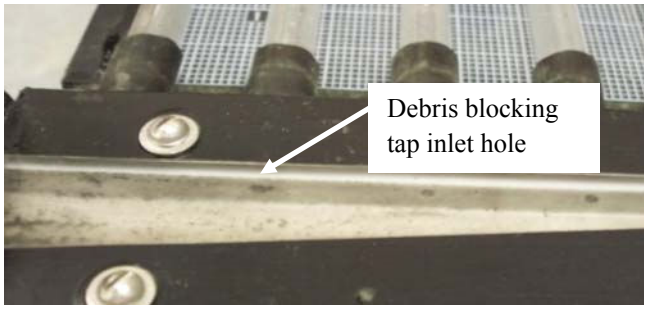

Fig. 9 Debris in Bernoulli apparatus

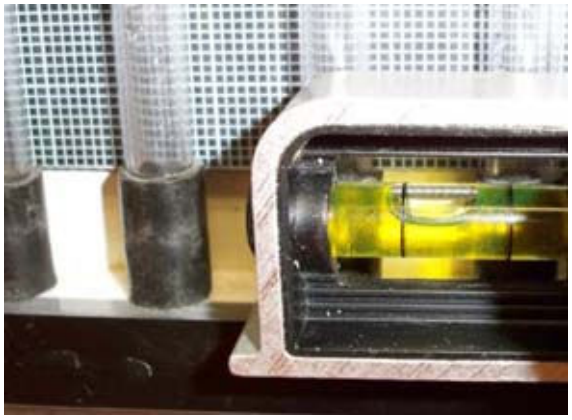

Fig. 10 Bernoulli apparatus with liquid level device

After taking steps to better control the experimental environment, the original experiment was run again in its entirety. Additionally, the initial experimental flow rates were matched when the experiment was repeated. Again, the raw manometer and flow rate data were analyzed, and the aforementioned calculations were performed. When comparing the two experiments, it was concluded that the changes in the experimental environment had little-to-no effect on the results. Negative head losses in the diverging half of the nozzle were still calculated, and the magnitude of the losses was almost identical in both cases. Now that several experimental factors could be ruled out, it could be hypothesized that the negative head losses were indeed the result of some strange fluid behavior that is not yet understood. The next step in this investigation was to focus on the fluid flow regime and attempt to achieve a completely laminar flow rate.

Laminar Flow Regime Experiments

In an attempt to achieve laminar flow rates with the Cussons test bench, the inlet tank was modified by removing the upper 25 mm portion of the overflow pipe. Additionally, a ball valve was added to the adjustable discharge pipe. This allowed for a much lower range of flow rates to be achieved, and the manometer readings could be easily read at the 25 mm inlet tank level. After running a number of initial trials, three runs were performed with the same procedure as the previous experiments, the subsequent raw data was collected, calculations were performed, and the results were analyzed. Again, pressure head was plotted against manometer tap and can be seen in figure 11. The overall loss in energy seems to be much less than in the turbulent cases, and this is expected for lower flow rates. It is important to note that the manometer scale is not accurate for flow rates lower than 0.9 LPM and is the limiting factor for the range of flow rates. The 0.92 LPM flow rate almost appears to be a horizontal line when plotted on the same scale as the turbulent runs. It should be noted that this run, 0.92 LPM, was the only one having Reynolds numbers at or below 2300 in the entire channel, including the throat (2375).

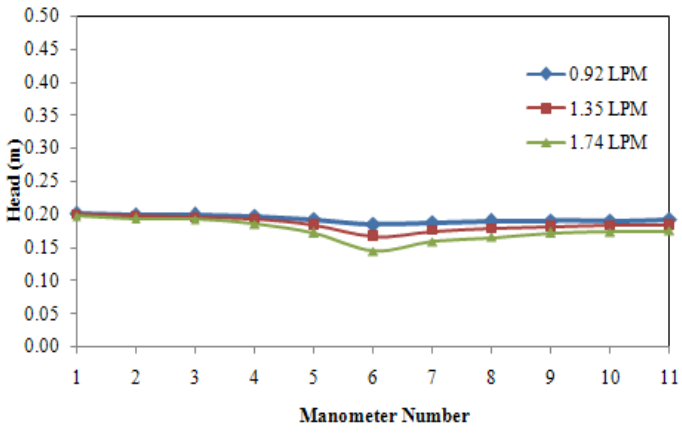

Fig. 11 Change in pressure head along channel length

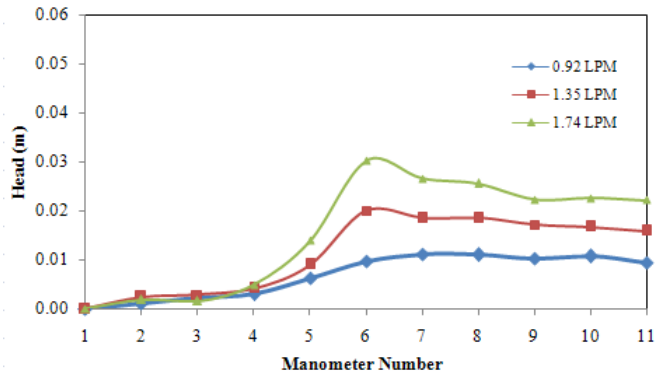

Fig. 12 Cumulative head losses (Laminar)

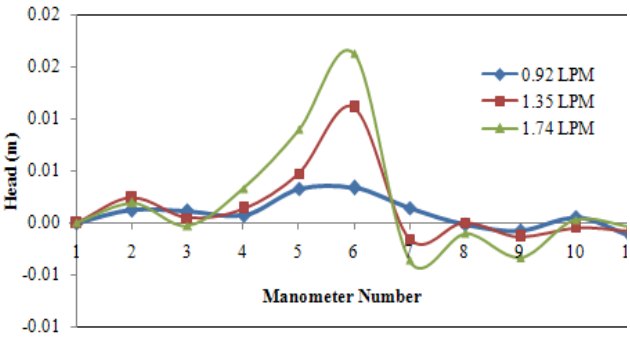

Fig. 13 Non-cumulative head losses (Laminar)

As shown in figure 12, the flow rates of 1.74 and 1.35 LPM follow the same trend as the turbulent flow rates; however, the 0.92 LPM flow rate shows a different trend after the throat. Head losses in the 0.92 LMP run seem to not become negative after the throat, but this could be caused by the inaccuracy of the measurement scale. Nonetheless, the negative head losses at tap 7 do seem to become closer to positive as the flow rate decreases, as shown in figure 13, particularly at the lowest flow rate. Overall the laminar trials do not yield results that can be used to explain the negative head loss phenomenon, but the trend indicates that the flow regime might have an impact.

Flow Visualizations

To better understand the behavior of the flow in the channel, several flow visualizations were performed in various flow rates. Black food coloring was diluted with an equal proportion of water and then injected into the inlet of the converging portion of the channel. A reservoir of ink was connected to the injector pipe with a clear tube, and initial calculations were performed to determine the optimal height for the reservoir. To clearly observe the nature of the flow, it was critical to match the ink to the fluid's flow rate.

Fig. 14 Laminar flow visualization

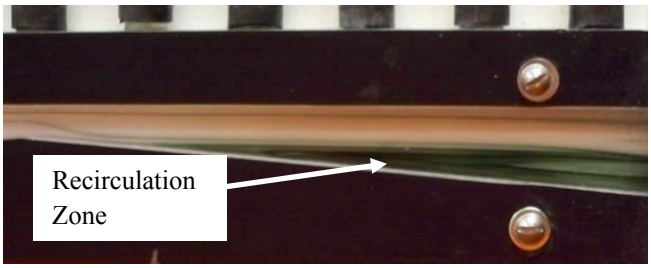

Fig. 15 Recirculation zone in diverging channel

Small variations in the ink height resulted in large changes in the ink flow rate, so the optimal flow rate was found through trial and error. In the assumed laminar flow rates, an undisturbed layer of ink can be seen over the entire channel length (figure 14). This observation was used to confirm that the calculated Reynolds numbers were correct along with the assumed flow regimes. One major discovery was made in the diverging half of the channel: during all flow rates, a clear recirculation zone can be observed (figure 15). This suggests that the fluid velocity is not slowing at the expected rate. The area above the recirculation zone is occupied by a distinct stream of fluid that seems to have the same flow area as in the throat of the nozzle. This discovery has some major implications in the way that the data is analyzed. To calculate the fluid velocity head, its kinetic energy is found as a function of its velocity. From the continuity equation, the fluid velocity is a function of the flow rate and the channel flow area. Thus, if the fluid is not expanding in the diverging half of the channel, its flow area remains close to that of the throat. This correction will serve to alter the predicted head losses and provide a more accurate result.

Theoretical Head Losses

To better understand the head losses in the system, the rates of energy conversion were plotted. Figures 16 and 17 show the differing rates of energy conversion in the converging and diverging sections of the channel. In the figures, pressure head was found using equation 1, and velocity head was found using equation 8. As defined by Bernoulli's equation, the rate of energy transfer from kinetic to pressure energy should be equal in both the diverging and converging sections of the channel. In the converging section, the magnitude of the slope is greater than in the diverging section. This suggests that the converging section is converting kinetic energy to pressure energy with more losses. The diverging section has a slope that suggests fewer losses occur.

Equation 8: $$V_{H_i} = \frac{V_i^2}{2 \cdot g}$$

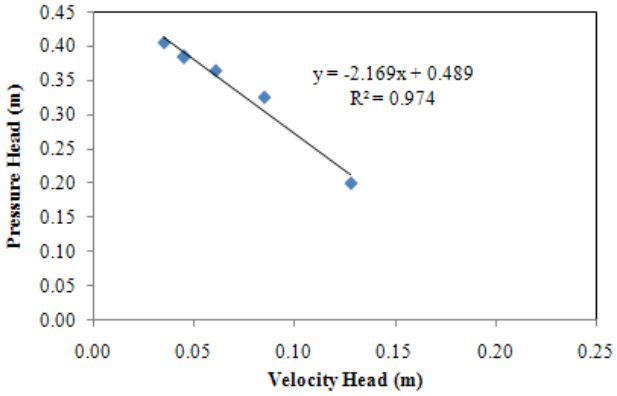

Fig. 16 Energy transfer taps 1-5

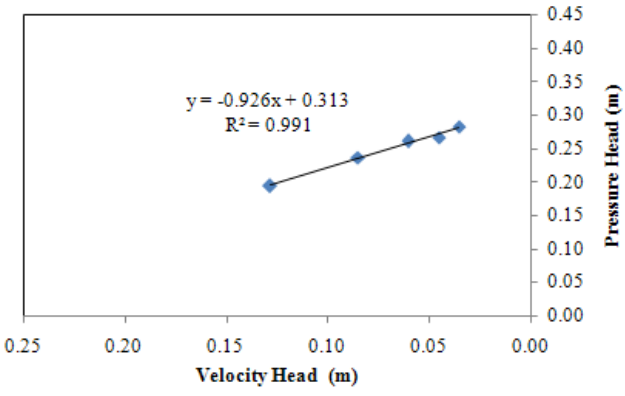

Fig. 17 Energy transfer taps 7-11

Equation 9: $$f_i = \frac{0.25}{\left[\log\left(\frac{1}{3.7\cdot(R_i/\varepsilon)} + \frac{5.47}{N_{R_i}^{0.9}}\right)\right]^2}$$

Equation 10: $$N_{R_i} = \frac{4\cdot V_i \cdot R_i \cdot \rho}{\eta}$$

Equation 11: $$R_i = \frac{[\Delta h_i + h_6]\cdot t}{2\cdot(h_i + t)}$$

Equation 12: $$\Delta h_i = \tan(\theta)\cdot \Delta L_{i-6}$$

Equation 13: $$HL_{TC_{i+1}} = HL_{T_i} + f_{i+1}\left[\left(\frac{\Delta L}{R_{i+1}\cdot 4}\right)\cdot\left(\frac{V_{i+1}^{\ 2}}{2\cdot g}\right)\right]$$

Figure 18 is a comparison of the experimental and theoretical head losses for the maximum flow rate. The head losses were found using equations 9 through 13 and are shown above. The change in length between manometer taps (ΔL) was measured to be 25 mm for all manometers, and a wall roughness (ε) of 3.0 x 10^{-7} m was used for plastic. Likewise, 4.29 degrees was used for both the converging and diverging angle of channel incline (θ). From taps 1 through 4, the losses appear to match almost flawlessly. In contrast, the head losses from taps 5 through 11 do not match as closely.

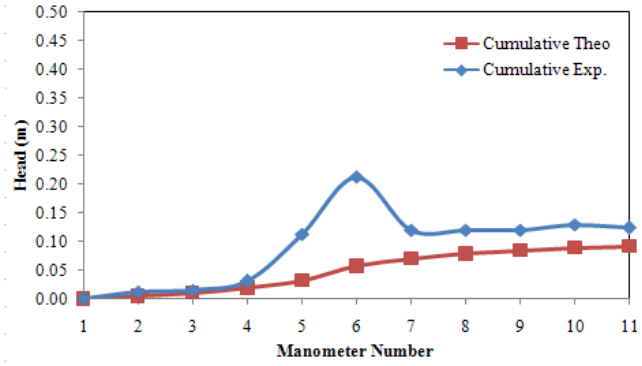

Fig. 18 Comparison of head losses

Next, using observations made during the flow visualization, two adjustments were made to the theoretical losses calculation. First, as previously mentioned, the fluid in the diverging section of the channel only experiences one-half of the wall friction. This is because a recirculation zone exists and the fluid is moving in a confined stream. Secondly, the flow area in the diverging section of the channel can be adjusted to not include the recirculation zone. The corrected formula for cumulative head losses (equation 14) can be seen below and was only used for taps 7 through11. By estimation, an adjusted theta of 2.0 degrees is used to calculate the actual flow area in the diverging portion of the channel (see equation 12). After making these adjustments, the theoretical head losses after the throat correlate well with experimental values as shown in figure 19. It can now be definitively concluded that the recirculation zone serves to reduce wall

friction and flow area in the diverging section of the channel. Furthermore, the throat of the channel can now be the focus for the rest of the investigation.

Equation 14: $$HL_{TC_{i+1}} = HL_{T_i} + \frac{1}{2} \cdot f_{i+1} \cdot \left[\left(\frac{\Delta L}{R_{i+1} \cdot 4} \right) \cdot \left(\frac{V_{i+1}^{\ 2}}{2 \cdot g} \right) \right]$$

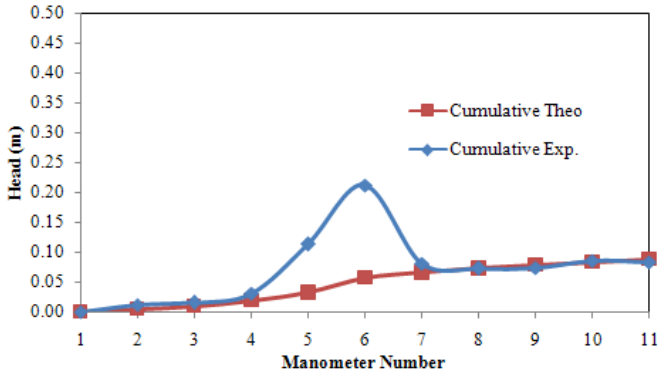

Fig. 19 Adjusted cumulative head losses

Numerical Simulations

Many 2D numerical simulations were attempted using FLUENT software in the laminar flow regime. Different boundary conditions, mesh refinements, and discretization methods were used. Currently more numerical simulations need to be done to accurately model what is happening in the channel. In some cases, the recirculation zone was observed, but the numerical solution may have contained errors indicated by the residuals plots. Moreover, a better understanding of the fluids behavior at the throat of the channel will come with more complex numerical simulations. Furthermore, simple 2D models may not explain the fluid behavior at the throat of the channel.

Conclusion

Several important discoveries were made during this investigation: Negative head losses in turbulent flow, a recirculation zone in the diverging channel section, and the throat of the channel were determined to be the cause of the strange results. Some difficulties were also encountered during the investigation process. Achieving laminar flow was difficult due to the accuracy of the manometer measuring scale. Nevertheless, a flow rate of 0.92 LPM was concluded to be laminar from calculated Reynolds numbers and showed positive head losses in the diverging half of the channel. However, this data may have been affected by the inaccuracy of the measurement scale; thus it cannot be used to make any definite explanations about the source of strange head loss results. On the contrary, after using various correction factors for

reduced wall friction and a decreased flow area, theoretical head losses correlated well with experimental losses with the exception of the throat. Overall, the fluid's behavior is highly complex in the throat and diverging section of the channel, and further experimental investigation, along with numerical simulations, are required to fully understand it. To summarize, numerical simulations can be an equal partner with theory and experimental data, but replicating the fluid flow correctly was found to be challenging. Lastly, with more numerical simulations and better-developed boundary conditions, the numerical results could help to explain the nature of the fluid flow at the throat.

References

1. Cussons, G. Instruction Manual-Investigation of Bernoulli's Theorem. Manchester, England : G. Cussons Ltd., 1991.

2. Mott, R. Applied Fluid Mechanics, 5TH Edition, Prentice Hall, 2005.